Korean J. Chem. Eng., **16**(3), 338-342 (1999)

Electrorheological Suspensions of Two Polarizable Particles

Young Dae Kim†, Guang Jin Choi, Sang Jun Sim and Young Sang Cho

Clean Technology Research Center, Korea Institute of Science and Technology,
P.O. BOX 131, Cheongryang, Seoul 130-650, Korea
(*Received 27 November 1998 • accepted 4 March 1999*)

Abstract-Bi-disperse Electrorheological (ER) suspensions of two polarizable particles of the same size are investigated to understand the ER behavior of poly-disperse suspensions composed of various polarizable particles. The electrostatic polarization model is employed to describe ER suspensions, and solutions to the equation of motion are obtained by dynamic simulation. Even with the applied electric field, metastable structures and sheared configurations at a shear rate of 0.01 and 10 s^{-1} show no inhomogeneous higher polarizable particle distributions (no higher polarizable particle cluster formation) regardless of the ratio of the two types of particles. The shear stress increases with the increase of the higher polarizable particle concentration both in the electrostatic force and hydrodynamic force dominant regions.

Key words : Electrorheology, Bi-disperse Suspensions, Electric Field

INTRODUCTION

The electrorheological (ER) response is defined as the dramatic change in rheological properties of a suspension of small particles due to the application of a large electric field transverse to the direction of flow. The structure is altered by the field-induced formation of fibrous aggregates aligned with the electric field. These effects are both rapid and reversible. The observation of a large ER effect was first reported by Winslow [1949].

The simplicity of engineering designs based on ER materials has facilitated the development of specifications for a broad range of devices, such as active engine mounts, shock absorbers, clutches, brakes, and adaptive structures [Winslow, 1949]. Although many ER devices have been brought successfully to the prototype stage, and despite much industrial activity in the U.S. and abroad, there are currently no commercially available devices. The main limitation of ER technology development is a lack of effective fluids [Weiss and Carlson, 1993]. Our inability to design effective fluids stems largely from insufficient understanding of the underlying mechanisms that control ER behavior. Understanding the phenomena underlying the ER effect and how each variable influences these phenomena as well as macroscopic behavior, will facilitate formulation of ER suspensions that satisfy application requirements.

In this paper, we investigate the ER behavior of bi-disperse particle suspensions composed of two different polarizable particles of the same particle size, employing the electrostatic polarization model.

MODEL AND SIMULATION METHOD

The microscopic model used here to describe ER suspensions has been presented in more detail elsewhere [Klingenberg et al., 1989; Klingenberg and Zukoski, 1990; Parthasarathy et al., 1996]. This model and other similar formalisms have been employed to demonstrate such aspects of ER as the formation of particulate chains that span the electrode gap, as well as the large increase in the apparent viscosity with increasing field strength [Klingenberg et al., 1989; Klingenberg and Zukoski, 1990; Parthasarathy et al., 1996]. Here we extend this model to account for polydisperse particle suspensions composed of various polarizable particles of the same particle size.

ER suspensions are treated as neutrally buoyant, hard, and uncharged dielectric spheres (complex dielectric constant e_p^*) immersed in a dielectric Newtonian continuous phase (complex dielectric constant e_c^*, viscosity h_c). All the spheres possess the same diameter, but can have different polarizabilities. Application of an electric field polarizes the spheres in different degrees depending on their polarizabilities, inducing electrostatic interactions between them, and between each particle and electrodes. The continuous phase is regarded as continuum ; its presence influences only the magnitude of the electrostatic interactions and hydrodynamic resistance on each sphere. For large particles under large electric fields, colloidal and Brownian forces are negligible [Marshall et al., 1989].

Ignoring inertia terms, the motion of sphere i not near an electrode is governed by

$$\mathbf{F}_i(\{\mathbf{R}_j\}) = 0, \tag{1}$$

where $\mathbf{F}_i(\{\mathbf{R}_j\})$ is the resultant force acting on sphere i due to the contributions described above, which depends on the positions of all of the spheres. Eq. (1) represents a coupled set of equations governing the motion of all the spheres not near electrodes. Solution of these equations requires explicit expressions for the forces.

Electrostatic forces are considered in the point dipole-limit. Employing the Maxwell-Wagner theory [Dukhin, 1970] for the

†To whom correspondence should be addressed.
E-mail : youngdae@kistmail.kist.re.kr

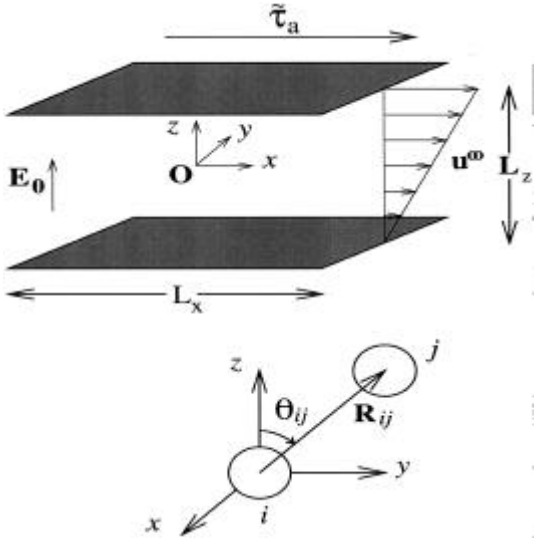

Fig. 1. Schematic diagrams showing the geometries of the sheared suspensions and sphere pairs. The bottom electrode is held fixed and the top electrode is displaced in the x-direction. R_{ij} is the center-to-center separation and q_{ij} is the angle between the line-of-centers and the applied electric field.

polarization of the disperse phase particles, the time averaged electrostatic force on sphere i at the origin of a spherical coordinate system due to sphere j at R_{ij}, q_{ij} (see Fig. 1) is given by

$$\mathbf{F}_{ij}^{el}(\mathbf{R}_{ij}, q_{ij}) = F_0[\text{Real}\ (b_i^{*k} b_j^{*l})]\ (d/R_{ij})^4\ [(3\cos^2 q_{ij} - 1)\ \mathbf{e}_r + \sin 2q_{ij}\ \mathbf{e}_q] \tag{2}$$

where

$$F_0 = (3/16)\ pe_0 e_c d^2 E_0^2, \tag{3}$$

$e_0 = 8.8542\times10^{-12}$ F/m, and $b^* = (e_p^* - e_c^*)/(e_p^* + 2e_c^*)$. $e^* = e - js/e_0 w_E$ is the complex dielectric constant, where e is the dielectric constant, s is the conductivity, d is the particle diameter, and w_E is the angular frequency of the applied electric field, $\mathbf{E} = E_0 \exp(jw_E t)\mathbf{e}_z$. The superscript on b is the particle polarizability index indicating each polarizable particle in a polydisperse suspension. For a bi-polarizable particle system, the index denotes either the higher or the lower polarizable particles.

The hydrodynamic force on sphere i is represented by Stokes' drag,

$$\mathbf{F}_i^{hyd}(\mathbf{R}_i) = 3ph_c\ d\ (\mathbf{u}^\infty(\mathbf{R}_i) - d\mathbf{R}_i/dt), \tag{4}$$

where $\mathbf{u}^\infty(\mathbf{R}_i)$ is the ambient velocity. The hard-sphere interactions between particles and between particles and electrode wall are approximated by short-range repulsive forces, as respectively,

$$\mathbf{F}_{ij}^{rep}(\mathbf{R}_{ij}) = -F_0[\text{Real}(b_i^{*k} b_j^{*l})]\ \exp(-k(R_{ij} - d)/d)\ \mathbf{e}_r, \tag{5}$$

$$\mathbf{F}_{i,\,wall}^{rep}(\mathbf{R}_i) = -F_0[\text{Real}(b_i^{*k} b_i^{*k})]\ \exp(-k(H_i - d/2)/d)\ \mathbf{n}, \tag{6}$$

where k^{-1} is the range of the repulsive force, $H_i = L_z/2 - |z_i|$, L_z is the electrode gap width, and $\mathbf{n}$ is the unit normal vector directed from the electrode into the suspension. For the results discussed below, $k = 10^2$.

Incorporating these forces into Eq. (1), the equation of motion for sphere i is written

$$3ph_c d\ d\mathbf{R}_i/dt = \sum_{j\neq i}\mathbf{F}_{ij}^{el}(R_{ij}, q_{ij}) + \sum_j \mathbf{F}_{ij}^{el}(R'_{ij}, q'_{ij}) + \sum''_{j\neq i}\mathbf{F}_{ij}^{rep}(R'_{ij}, q'_{ij}) + 3ph_c d\ \mathbf{u}^\infty(\mathbf{R}_j). \tag{7}$$

The primes in the second summation indicate the electrostatic force between sphere i and the image of sphere j; these forces are summed over all images of all spheres, including those of sphere i. The double prime in the third summation indicates that repulsive forces are evaluated between sphere i and all spheres $j \neq i$, as well as between sphere i and the electrodes. Eq. (7) governs the motion of spheres not near an electrode surface. Spheres within $d_w = 0.05d$ of an electrode are considered stuck and assume the lateral velocity of the electrode. This sticking condition is based on experimental observation [Klingenberg and Zukoski, 1990].

The equation of motion is made dimensionless with the following length, force, and time scales:

$$l_{scale} = d,\ F_{scale} = (3/16)\ pe_0\ e_c\ d^2\ b_{base}^2\ E_0^2,$$
$$t_{scale} = 16h_c/(e_0\ e_c b_{base}^2\ E_0^2),$$

where $b^2 \equiv b^*\bar{b}^*$, $\bar{b}^*$ is the complex conjugate of b^*, and b_{base}^* is the effective relative polarizability of the base particles. The equation of motion in dimensionless form for sphere i not near an electrode is written

$$d\mathbf{r}_i^*/dt^* = \sum_{j\neq i}\mathbf{f}_{ij}^{el*} + \sum_j \mathbf{f}'^{el*}_{ij} + \sum''_{j\neq i}\mathbf{f}_{ij}^{rep*} + \mathbf{u}^{\infty*}(\mathbf{r}_i^*), \tag{8}$$

where the asterisks denote dimensionless quantities. The equations governing the motion of stuck spheres are written

$$dx_i^*/dt^* = u_{x,elec}^*, \quad dy_i^*/dt^* = u_{y,elec}^* \tag{9}$$

$$dz_i^*/dt^* = \sum_{j\neq i} f_{z,ij}^{el*} + \sum_j f'^{el*}_{z,ij} + \sum''_{j\neq i} f_{z,ij}^{rep*} + u_{z,elec}^*, \tag{10}$$

where u_k is the k^{th} component of the electrode velocity. Here, we consider start-up of steady shear flow,

$$\mathbf{u}^{\infty*}(\mathbf{r}_i^*) = \begin{cases} 0 & t \le 0, \\ \gamma^{o*}(z_i^* + L_z^*/2)\mathbf{e}_x & t > 0, \end{cases} \tag{11}$$

where g^{o*} is the dimensionless shear rate. We also limit discussion to the cases where the electrostatic and deformation time scale are decoupled, i.e., $g^{o*} << w_E^*$ or $w_E^* = 0$ (dc), where w_E^* is the dimensionless electric field frequency.

Eqs. (8)-(10) are solved by the dynamic simulation technique. N spheres are placed between electrodes at $z^* = \pm L_z^*/2$, and within periodic boundaries at $z^* = \pm L_z^*/2$, $x^* = \pm L_x^*/2$, $y^* = \pm L_y^*/2$. Simulations in two dimensions are performed by placing all spheres in a plane, $y^* =$ constant. Spheres are placed randomly or in a prescribed configuration. Eqs. (8)-(10) are integrated numerically for each sphere by using Euler's method, with a time step $Dt^* \le 10^{-3}$. Forces are evaluated within cutoff radius $r_c^* = L_z^*/2$, employing a neighbor list with a cutoff radius $r_l^* = r_c^* + 0.2$ [Allen and Tildesley, 1989]. For rheological simulations, a static metastable structure is first obtained by integrating the equations of motion under no flow until motion ceases. After the metastable structure is obtained, simulation under the desirable flow is begun.

Once the sphere positions have been determined as a func-

tion of time, the rheological properties can be evaluated. The total stress is conveniently expressed as a sum of direct electrostatic and hydrodynamic contributions [Klingenberg, 1993]

$$s^{total} = s^{E} + s^{H}. \tag{12}$$

This distinction between the contributions is arbitrary. Since elasticity arises only from non-hydrodynamic forces [Russel et al., 1989], we consider only the direct electrostatic contribution to the shear stress,

$$\sigma^*_{xz}(t^*) = -1/V^* \sum_i z_i^* f_{xi}^{total*}(\{\mathbf{r}_j^*(t^*)\}), \tag{13}$$

where $s^*_{xz}(t^*)$ is the dimensionless time-dependent shear stress acting in the x-direction on a plane normal to the z-direction, $f_{xi}^{total*}(\{\mathbf{r}_j^*(t^*)\})$ is the total dimensionless electrostatic plus short-range repulsive force acting on sphere i in the x-direction, and V^* is the dimensionless suspension volume.

RESULTS AND DISCUSSIONS

Simulations are performed to investigate the ER behavior of bi-disperse suspensions of bi-polarizable particles of the same size and to relate the ER behavior to the particle distribution change. Sakurai et al. [1996] observed a significant dip in the shear stress under a dc electric field as the concentration of the higher conductivity particles increased. They explained the reduction in the shear stress by the higher conductivity particle cluster formation (i.e., inhomogeneity in particle distributions). In their experiments, the Mason numbers under their experimental conditions were less than 1 (i.e., the electrostatic force is dominant over the hydrodynamic force).

When the hydrodynamic force is dominant over the electrostatic force (Mason number > 1), particles will be uniformly distributed without the higher polarizable particle cluster formation in bi-disperse suspensions. The shear stress will increase with the increase of the higher particle concentration. When the electrostatic force is dominant over the hydrodynamic force (Mason number < 1), we can speculate that if particle distributions are not uniform (higher polarizable particle cluster formation) due to the different induced dipole interactions between particles of different polarizabilities, the shear stress may show an abnormal behavior (such as a dip in the shear stress as the higher conductivity particle concentration increases as observed by Sakurai et al.). Otherwise, the shear stress will increase with the higher polarizable particle concentrations.

Steady shear flow simulations in two dimensions (N = 250, $L_x^* = 50$, $L_z^* = 10$, $g^{o*} = 0.01$ or 10.0) were performed with six initial configurations of the various higher polarizable particle concentrations (i.e., 0, 20, 40, 60, 80, and 100 % of the higher polarizable particles). Suspensions are composed of bi-polarizable particles (having either different dielectric constants or conductivities) of the same particle size. The particles having the higher polarizability (dielectric constant or conductivity) are referred to as the higher particles and those having a lower one are referred to as the base particles. As mentioned, we limit discussion to the cases where the electrostatic and deformation time scale are decoupled, i.e., $g^{o*} << w_E^*$ or $w_E^* = 0$ (dc). In these limits, the effective relative polarizability, b^*, is determined by the mismatches of either dielectric constants [$b^* = (e_p - e_c)/(e_p + 2e_c)$ when $g^{o*} << w_E^*$ *or* $w_E^* \to \infty$] or conductivities [$b^* = (s_p - s_c)/(s_p + 2s_c)$ when $w_E^* = 0$ (dc)]. In either case, the ER behavior is the same if the dielectric constant ratio and the conductivity ratio between the higher and base particles are the same. The dielectric constant ratio (or conductivity ratio) between the high and base particles is 8.98 in this discussion.

Initially, six random configurations of different higher particle concentrations are generated. A static metastable structure for each random configuration is first obtained by integrating the equations of motion under no flow until motion ceases. After the metastable structure is obtained, simulation under the desirable flow is begun. Simulations are performed on two dimensionless shear rates (0.01 and 10 s^{-1}) for six metastable structures. The shear rate of 0.01 s^{-1} is chosen to investigate the ER behavior when the electrostatic force is dominant over the hydrodynamic force (Mason number << 1), while the shear rate of 10 s^{-1} is chosen to investigate the ER behavior when the hydrodynamic force is dominant (Mason number >> 1).

Figs. 2 and 3 present configurations of bi-disperse suspensions of 20 % and 60 % higher particle concentrations, respectively : (a) initial random structure, (b) metastable structure under an electric field, and (c) sheared structures under the shear rates of 0.01 and (d) 10 s^{-1}. Both metastable structures [Fig. 2(b) and Fig. 3(b)] evolved from initial random structures do not show any particular inhomogeneity in the higher

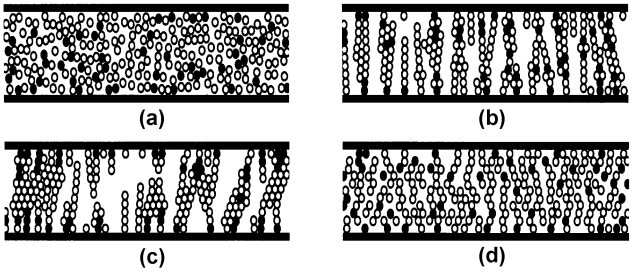

Fig. 2. Configurations of 20 % higher particle concentration. (a) initial random configuration, (b) metastable structure under an electric field, (c) at the shear rate of 0.01 s^{-1}, and (d) at the shear rate of 10 s^{-1}. Black spheres are the higher polarizable particles and hollow ones are the base particles.

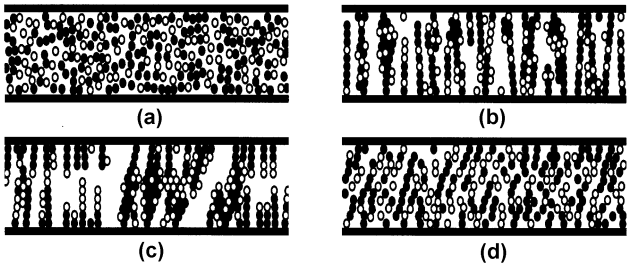

Fig. 3. Configurations of 60 % higher particle concentration. (a) initial random configuration, (b) metastable structure under an electric field, (c) at the shear rate of 0.01 s^{-1}, and (d) at the shear rate of 10 s^{-1}. Black spheres are the higher polarizable particles and hollow ones are the base particles.

particle distributions (i.e., no particular higher particle cluster formation), indicating that non-uniform induced dipole interactions between particles do not lead to an inhomogeneous higher particle distribution. However, it is observed that the higher particles have more populations at the electrode wall compared to the initial higher particle concentrations for all suspensions of various higher polarizable particle concentrations. The phenomena seem to arise from the stronger interactions of higher polarizable particles with the electrode wall due to their higher polarizability than the base particles. The observed no inhomogeneous higher particle distributions in metastable structures of bi-disperse suspensions suggest that the shear stress may increase with the higher particle concentrations.

The sheared configurations at the shear rate of 0.01 s^{-1} [Fig. 2(c) and Fig. 3(c)] show no particular inhomogeneous higher particle distributions, consistent with the metastable structures. These no particular inhomogeneities in the higher particle distributions in metastable structures and sheared configurations at the shear rate of 0.01 s^{-1} do not agree with Sakurai et al.'s speculation of the high particle cluster formation, leading to the notion that the observed shear stress reduction may not arise from preferred interactions between the higher polarizable particles.

The shear stress as a function of strain at the shear rate of 0.01 s^{-1} is investigated for various higher particle concentrations and presented in Fig. 4. For all bi-disperse suspensions of various higher particle concentrations, the shear stress showed an initial increase upon the applying of the shear of 0.01 s^{-1} and reached a steady state. The initial increase of the shear stress arises from the rearrangement of particle configurations under the applied shear rate. The steady shear stresses increase with the higher particle concentrations, expected from the homogeneous metastable structures and sheared particle distributions [Fig. 2(b) and (c), and Fig. 3(b) and (c)]. At a shear rate of 10 s^{-1}, the spanned structures are completely destroyed by the dominant hydrodynamic force, and particle distributions are homogeneous [Fig. 2(d) and Fig. 3(d)]. It is observed that the shear stress also increases with the higher particle concentrations, consistent with the homogeneous particle distributions.

The steady shear stress as a function of the higher particle concentrations is summarized in Fig. 5 for both high and low shear rates. Regardless of the applied shear stress, the shear stress increases with the increase of the higher particle concentrations, showing no abnormal shear stress behavior, consistent with the observed homogeneous metastable structures and sheared particle distributions. To illustrate the linear ER behavior with the increase of the higher particle concentrations, the viscosity as a function of the higher particle concentrations is shown in Fig. 6. As expected, the bi-disperse suspension viscosity increases linearly with the higher particle concentra-

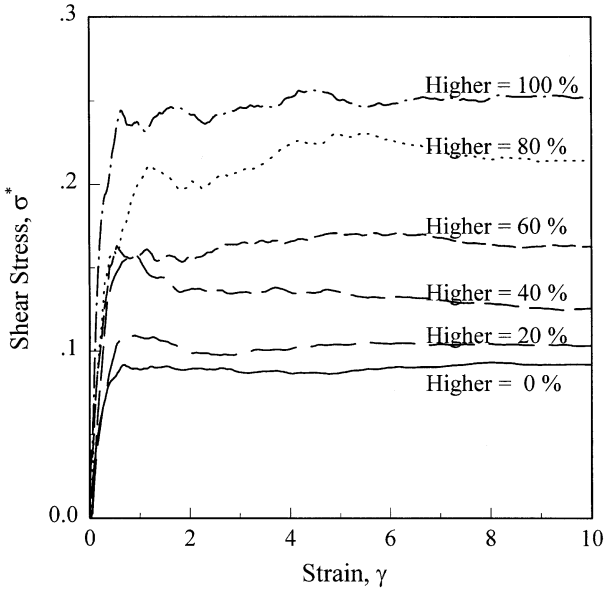

Fig. 4. Shear stress as a function of strain at the shear rate of 0.01 s^{-1} for several higher particle concentrations.

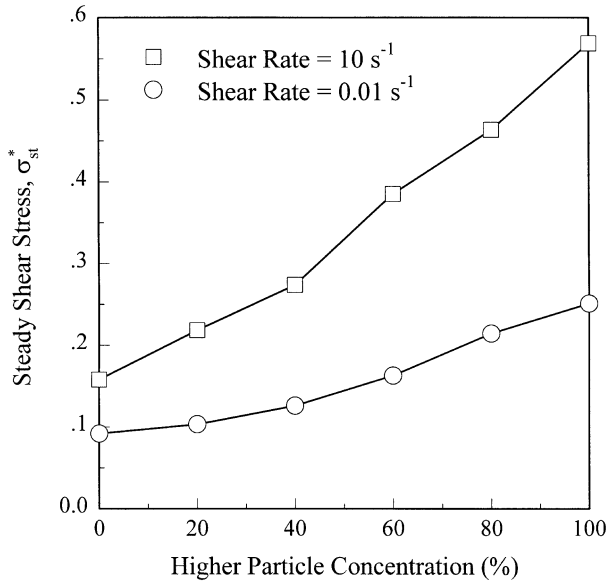

Fig. 5. Steady shear stress as a function of the higher particle concentration at the shear rate of 0.01 and 10 s^{-1}.

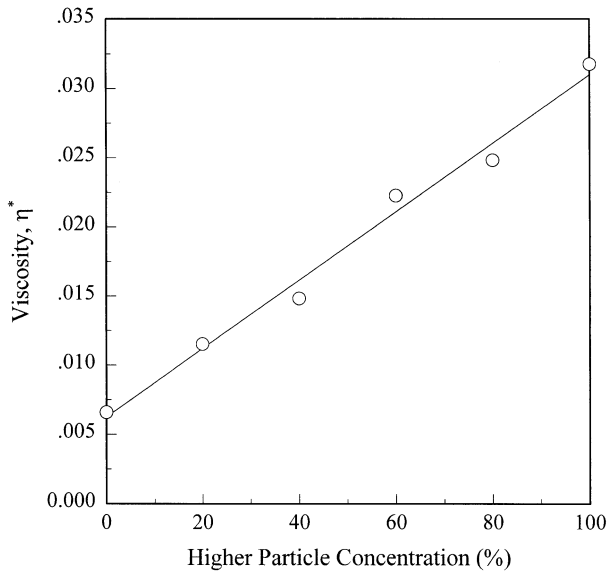

Fig. 6. Apparent suspension viscosity as a function of the higher particle concentration.

tions.

The above results indicate that there is no distinct higher particle cluster formation (i.e., no inhomogeneous higher polarizable particle distributions) even if the electrostatic force is dominant over the hydrodynamic force. The shear stress increases with the higher particle concentrations both in the electrostatic force and hydrodynamic force dominant regions, showing no abnormal ER behavior due to the non-uniform induced dipole interactions between various polarizable particles. Furthermore, for Sakurai et al.'s system, $b \approx 1$ for various dipole interactions between the higher and base particles (i.e., induced dipole interaction differences are almost negligible), suggesting that the abnormal shear stress behavior may not arise from the electrostatic polarization. For conducting particle systems, there is another competing mechanism such as conduction through particle strands in addition to the electrostatic polarization [Kim and Klingenberg, 1996, 1997].

CONCLUSIONS

Bi-disperse ER suspensions of two polarizable particles of the same size are investigated. Under the applied electric field, metastable structures and sheared configurations at the shear rate of 0.01 and 10 s^{-1} show no inhomogeneous higher polarizable particle distributions regardless of the higher particle concentrations. The shear stress increases with the increase of the higher polarizable particle concentration both in the electrostatic force and hydrodynamic force dominant regions, showing no abnormal ER behavior due to the mixing of various polarizable particles.

REFERENCES

Allen, M. P. and Tildesley, D. J., "Computer Simulations of Liquids," Oxford Univ. Press, New York (1991).

Bonnecaze, R. T. and Brady, J. F., "Dynamic Simulations of an Electrorheological Fluid," *Journal of Chemical Physics*, **96**, 2138 (1992).

Dukhin, S. S., "Dielectric Properties of Disperse Systems," *Journal of Surface and Colloid Science*, **3**, 83 (1970).

Kim, Y. D. and Klingenberg, D. J., "The Nonlinear Behavior of Surfactant-activated Electrorheological Suspensions," **14**, 23 (1997).

Kim, Y. D. and Klingenberg, D. J., "Two Roles of Nonionic Surfactants on the Electrorheological Response," *Journal of Colloid and Interface Science*, **183**, 568 (1996).

Klingenberg, D. J. and Zukoski, C. F., "Studies on the Steady-State Behavior of Electrorheological Suspensions," *Langmuir*, **6**, 15 (1990).

Klingenberg, D. J., "Simulation of the Dynamic Oscillatory Response of Electrorheological Suspensions ; Demonstration of a Relaxation Mechanism," *Journal of Rheology*, **37**, 199 (1993).

Klingenberg, D. J., van Swol, F. and Zukoski, C. F., "Dynamic Simulation of Eelectrorheological Suspensions," *Journal of Chemical Physics*, **91**, 7888 (1989).

Marshall, L., Goodwin, J. W. and Zukoski, C. F., "Effect of Electric Fields on the Rheology of Nonaqueous Concentrated Suspensions," *Journal of Chemical Society Faraday Transaction I*, **85**, 2785 (1989).

Parthasarathy, M., Kim, Y. D. and Klingenberg, D. J., "Nonlinear Rheological Properties of Electrorheological Suspensions," In Proceedings of 5th World Congress of Chemical Engineering, Sandiego, California (1996).

Russel, W. D., Saville, D. A. and Schowalter, W. R., "Colloidal Dispersions," Cambridge Univ. Press, Cambridge (1989).

Sakurai, R., See, H. and Saito, T., "The Effect of Blending Particles with Different Conductivity on Electrorheological Properties," *Journal of Rheoloy*, **40**, 395 (1996).

Weiss, K. D. and Carlson, J. D., "Material Aspects of Electrorheological Systems," *Journal of Intelligent Systems and Structures*, **4**, 13 (1993).

Winslow, W. M., "Induced Fibration of Suspensions," *Journal of Applied Physics*, **20**, 1137 (1949).